ELSEVIER

Journal of Alloys and Compounds 427 (2007) 171–175

Journal of ALLOYS AND COMPOUNDS

www.elsevier.com/locate/jallcom

A new Ti–Zr–Hf–Cu–Ni–Si–Sn bulk amorphous alloy with high glass-forming ability

Y.J. Huang [a], J. Shen [a,*], J.F. Sun [a], X.B. Yu [b,*]

[a] *School of Materials Science and Engineering, Harbin Institute of Technology, Harbin 150001,China*
[b] *Lab of Energy Science and Technology, Shanghai Institute of Microsystem and Information Technology, Chinese Academy of Sciences, Shanghai 200050, China*

Received 22 December 2005; received in revised form 5 March 2006; accepted 8 March 2006
Available online 18 April 2006

Abstract

The effect of Sn substitution for Cu on the glass-forming ability was investigated in $Ti_{41.5}Zr_{2.5}Hf_5Cu_{42.5-x}Ni_{7.5}Si_1Sn_x$ ($x = 0$, 1, 3, 5, 7) alloys by using differential scanning calorimetry (DSC) and X-ray diffractometry. The alloy containing 5% Sn shows the highest glass-forming ability (GFA) among the Ti–Zr–Hf–Cu–Ni–Si–Sn system. Fully amorphous rod sample with diameters up to 6 mm could be successfully fabricated by the copper mold casting $Ti_{41.5}Zr_{2.5}Hf_5Cu_{37.5}Ni_{7.5}Si_1Sn_5$ alloy. The activation energies for glass transition and crystallization for $Ti_{41.5}Zr_{2.5}Hf_5Cu_{37.5}Ni_{7.5}Si_1Sn_5$ amorphous alloy are both larger than those values for the Sn-free alloy. The enhancement in GFA and thermal stability after the partial replacement of Cu by Sn may be contributed to the strong atomic bonding nature between Ti and Sn and the increasing of atomic packing density. The amorphous $Ti_{41.5}Zr_{2.5}Hf_5Cu_{37.5}Ni_{7.5}Si_1Sn_5$ alloy also possesses superior mechanical properties.

Keywords: Bulk amorphous alloy; Glass-forming ability; Thermal stability; Titanium alloy

1. Introduction

In recent years, much attention has been paid to explore Ti-based bulk amorphous alloys (BAAs) due to their high specific strength and low cost [1–11]. Development of Ti-based BAAs is expected to significantly expand the application fields of BAAs. To date, a number of Ti-based bulk glass-forming alloys, such as Ti–Cu–Ni–(Sn or Sb) [1], Ti–Cu–Ni–Si–B [2,3], Ti–Zr–Ni–Cu–Sn [4] and Ti–Cu–Ni–Zr–Al–Si–B [5], (Ti, Zr)–(Cu, Ni) [6] have been synthesized by the copper casting method. Indeed, the Ti-based amorphous alloys have already shown to form glassy rods with maximum diameters up to 6–14 mm [7–9]. However, these amorphous alloys with critical thickness larger than 5 mm usually contain toxic element (such as beryllium). It is of scientific and technological interest to synthesize a new Ti-based bulk amorphous alloy free of toxic element, but with low density and high strength.

Ma et al. [11] have recently tried to improve the glass-forming ability (GFA) of a eutectic alloy $Ti_{50}Cu_{42.5}Ni_{7.5}$ by substituting Ti with appropriate amounts of Zr and Hf as well as a minor amount of Si and succeeded in synthesizing Ti-based BAAs with maximum diameters up to 5 mm for $Ti_{41.5}Zr_{2.5}Hf_5Cu_{42.5}Ni_{7.5}Si_1$ by using the copper mold casting.

In this paper, the effect of a seventh alloying element Sn on glass formation in $Ti_{41.5}Zr_{2.5}Hf_5Cu_{42.5}Ni_{7.5}Si_1$ was investigated. Bulk glassy alloy sample with a diameter up to 6 mm was successfully prepared for the $Ti_{41.5}Zr_{2.5}Hf_5Cu_{37.5}Ni_{7.5}Si_1Sn_5$ alloy. The crystallization kinetics of this amorphous alloy was assessed by means of differential scanning calorimetry (DSC). The mechanical properties of this alloy were also tested.

2. Experimental procedure

Alloy ingots, with nominal composition $Ti_{41.5}Zr_{2.5}Hf_5Cu_{42.5-x}Ni_{7.5}Si_1Sn_x$ ($x = 0$, 1, 3, 5, 7) (at.%), were prepared by arc melting a mixture of pure elements with a purity above 99.9% in a titanium–gettered argon atmosphere. To reach a high homogeneity, the alloy ingots were remelted several times. Rapidly solidified ribbon specimens were prepared by remelting the alloys in quartz tubes, and ejecting onto a Cu wheel rotating with a surface velocity of 40 m/s. The resulting ribbons have a thickness of about 40 μm and a width of about 2 mm.

* Corresponding authors. Tel.: +86 451 86418317; fax: +86 451 86415776.
E-mail addresses: junshen@hit.edu.cn (J. Shen), yuxuebin@hotmail.com (X.B. Yu).

0925-8388/$ – see front matter © 2006 Elsevier B.V. All rights reserved.
doi:10.1016/j.jallcom.2006.03.006

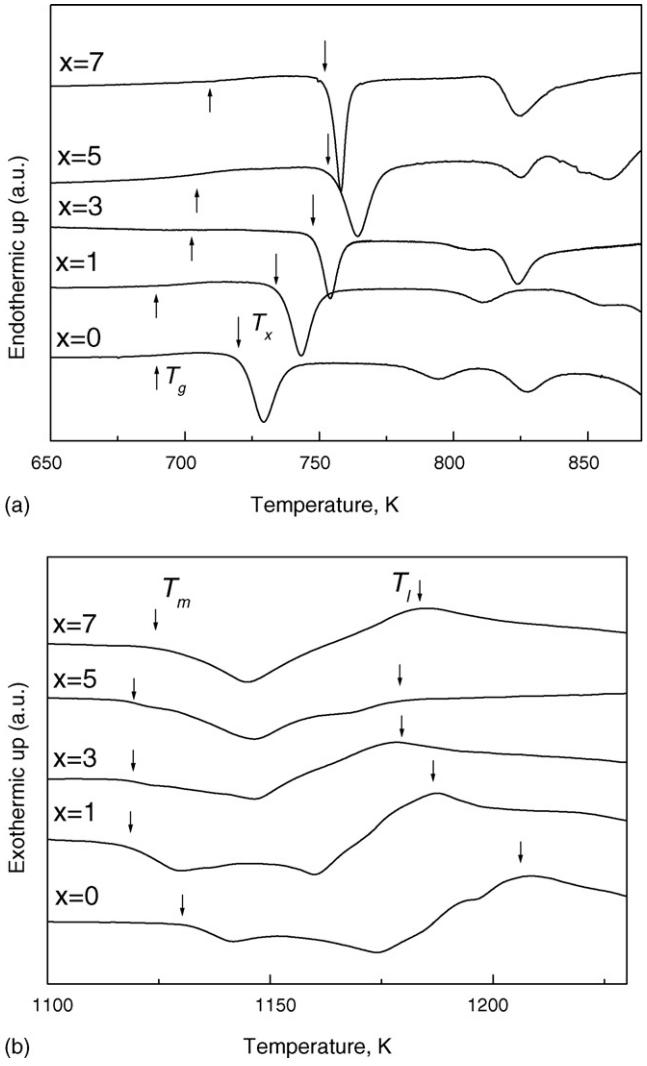

Fig. 1. DSC (a) and DTA (b) curves obtained from the as-cast $Ti_{41.5}Zr_{2.5}Hf_5Cu_{42.5-x}Ni_{7.5}Si_1Sn_x$ ($x = 0$, 1, 3, 5, 7) alloys at a heating rate 20 K/min. The samples are 1 mm in diameter.

Bulk amorphous alloys were prepared by drop casting into a copper mold and the obtained cylindrical samples have diameters up to 8 mm. The amorphous nature of the rod and ribbon samples was confirmed by X-ray diffraction technique with Cu K_α radiation. To determine the glass transition temperature, T_g, onset crystallization temperature, T_x, peak crystallization temperature, T_p, and other thermal properties of the alloys, thermal analysis was performed using differential scanning calorimetry (DSC) with heating rates from 20 to 100 K/min in a flow of purified argon gas. The density of the as-cast samples was measured by the Archimedean method at room temperature. Vickers hardness was tested by using the HVS-1000 digital-display micro-hardness tester. From the as-cast rods, cylindrical samples with a diameter of 3 mm and a height of 6 mm were prepared for the uniaxial compression tests at room temperature, which were conducted on an Instron 5500 mechanical instrument under an initial strain rate of 4×10^{-4}/s.

3. Results and discussion

Fig. 1 shows the DSC and DTA curves obtained from 1 mm as-cast samples for $Ti_{41.5}Zr_{2.5}Hf_5Cu_{42.5-x}Ni_{7.5}Si_1Sn_x$ ($x = 0$, 1, 3, 5, 7) alloys at a heating rate of 20 K/min. A distinct glass transition followed by a wide supercooled liquid region and several exothermic peaks due to a multi-stage crystallization were observed in the DSC traces for all alloys. The glass transition temperature, T_g, onset temperature of crystallization, T_x, onset melting temperature, T_m, liquidus temperature, T_l, and other deduced characteristic thermodynamic parameters are summarized in Table 1. The glass transition temperatures shift to higher temperatures with increasing Sn content. However, the onset temperatures of crystallization increase with increasing Sn content up to 5 at.% and then decrease with further increasing Sn content. As shown in Fig. 1(b) and Table 1, the alloy containing 5% Sn shows the lowest liquidus temperature.

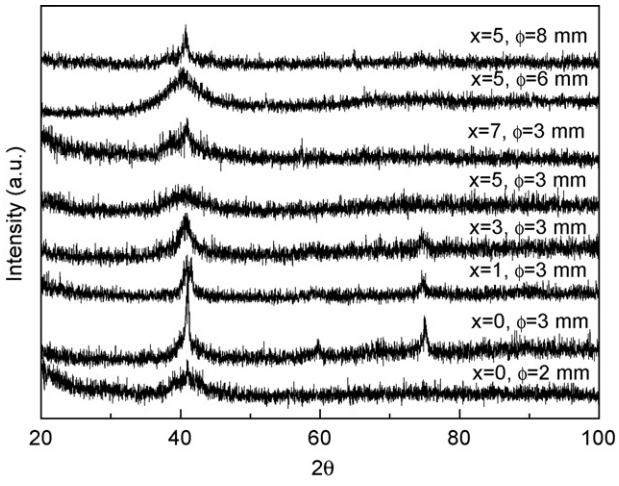

Fig. 2. XRD patterns of the as-cast $Ti_{41.5}Zr_{2.5}Hf_5Cu_{42.5-x}Ni_{7.5}Si_1Sn_x$ ($x = 0$, 1, 3, 5, 7) alloys with diameters ranging from 2 to 8 mm.

Hitherto, several parameters have been used to reflect the GFA of metallic glasses. The reduced glass transition temperature (T_{rg}) defined by Turnbull as the ratio between the glass transition (T_g) and liquidus (T_l) temperature has been successfully used to evaluate the GFA of various amorphous alloys [12]. The temperature interval $\Delta T_x = T_x - T_g$ referred to as the supercooled liquid region, was also once regarded as a useful parameter of GFA [13]. Furthermore, Lu et al. proposed a parameter $\gamma = T_x/(T_g + T_l)$, which was obtained by simple additive assumption of devitrification tendency of a glass and suppression of crystallization during solidification, to predict the GFA for various glass forming systems [14]. Recently, Chen et al. defined a new parameter $\delta = T_x/(T_l - T_g)$, derived from the classical nucleation and growth theory, to evaluate the GFA of a metallic glass [15]. In this study, to evaluate the GFA of the alloys, the values of ΔT_x, δ, γ, and T_g/T_l for the alloys were also included in the Table 1. In view of the highest ΔT_x, δ, γ, and T_g/T_l, it can be speculated that the alloy with 5% Sn in place of Cu has the highest GFA compared to other alloys with different Sn contents.

Fig. 2 shows the XRD patterns obtained from as-cast rods of $Ti_{41.5}Zr_{2.5}Hf_5Cu_{42.5-x}Ni_{7.5}Si_1Sn_x$ ($x = 0$, 1, 3, 5, 7) alloys. For the Sn-free base alloy (i.e. $Ti_{41.5}Zr_{2.5}Hf_5Cu_{42.5}Ni_{7.5}Si_1$), the broadened XRD pattern of the 2 mm sample suggests its amorphous nature, but by a careful examination, there still exist some small crystalline peaks in the XRD pattern, at the same time, sev-

Table 1
Thermal properties of the as-cast $Ti_{41.5}Zr_{2.5}Hf_5Cu_{42.5-x}Ni_{7.5}Si_1Sn_x$ ($x = 0, 1, 3, 5, 7$) alloys with a heating rate of 20 K/min

Alloy (x)	T_g (K)	T_x (K)	ΔT_x (K)	T_m (K)	T_l (K)	T_g/T_l	γ	δ
0	684.56	719.91	35.35	1131.74	1206.17	0.568	0.381	1.380
1	684.79	733.35	48.56	1117.87	1187.00	0.577	0.392	1.460
3	692.97	755.57	62.60	1117.03	1177.12	0.589	0.404	1.561
5	693.33	757.52	64.19	1116.66	1176.07	0.590	0.405	1.569
7	697.65	752.27	54.62	1124.49	1183.32	0.589	0.400	1.549

eral sharp crystalline peaks are visible in the XRD pattern of the 3 mm sample, indicating that the maximum diameter for glass formation is about 2 mm. In contrast, for the alloy containing 5% Sn, there are no Bragg peaks corresponding to crystalline phases in the XRD patterns taken from its 3 and 6 mm samples, but sharp Bragg peaks superimposed on the broad halo peak for the 8 mm sample can be observed, demonstrating that the maximum diameter for glass formation of the 5% Sn containing alloy with mostly amorphous structure can reach up to 6 mm. To our knowledge, 6 mm is the largest glassy sample size reported to date for Ti-BAAs without toxic element (such as beryllium).

Fig. 3 presents the DSC traces in the continuous heating mode with a heating rate of 40 K/min for the amorphous $Ti_{41.5}Zr_{2.5}Hf_5Cu_{37.5}Ni_{7.5}Si_1Sn_5$ ribbon sample and 6 mm-diameter rod sample. The glass transition temperature and the onset temperature of crystallization for the 6 mm-diameter sample were exactly same as those for the ribbon sample within the experiment error. Furthermore, total exothermic heats during crystallization in the ribbon and the 6 mm-diameter samples were nearly same, i.e., −87 J/g for the ribbon sample and −85 J/g for the rod sample. The selected area electron diffraction (SAED) pattern (inset in Fig. 3) for the 6 mm-diameter sample consists of a diffuse halo ring. All of these data confirm that the 6 mm sample is mostly amorphous. For the base alloy ($x = 0$), the maximum diameter achievable in this study is about 2 mm (see Fig. 2), which is smaller than that reported by Ma et al.

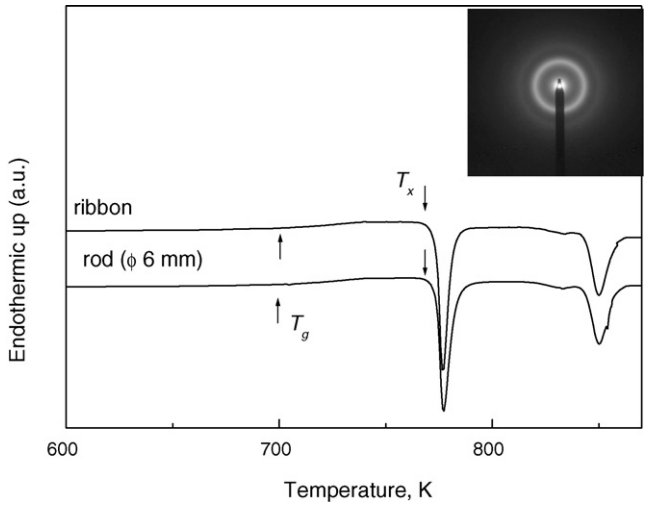

Fig. 3. DSC curves of rod with a diameter of 6 mm and ribbon sample for $Ti_{41.5}Zr_{2.5}Hf_5Cu_{37.5}Ni_{7.5}Si_1Sn_5$ amorphous alloys at a heating rate 40 K/min. The inset shows the SAED pattern of a 6 mm-diameter glassy sample for the $Ti_{41.5}Zr_{2.5}Hf_5Cu_{37.5}Ni_{7.5}Si_1Sn_5$ alloy.

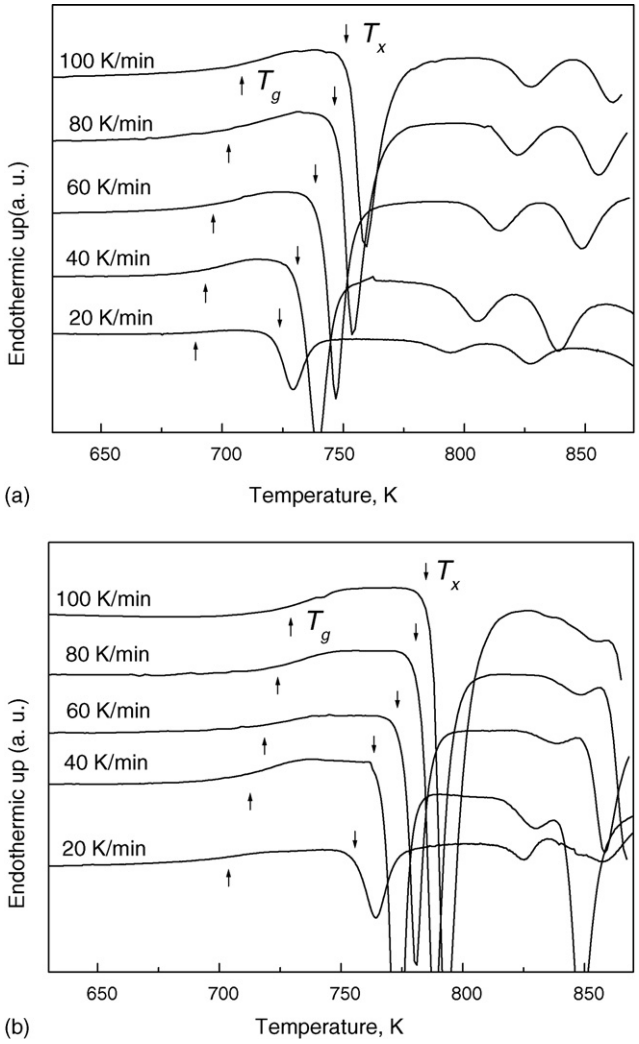

Fig. 4. DSC curves of $Ti_{41.5}Zr_{2.5}Hf_5Cu_{42.5}Ni_{7.5}Si_1$ (a) and $Ti_{41.5}Zr_{2.5}Hf_5Cu_{37.5}Ni_{7.5}Si_1Sn_5$ (b) amorphous alloys at various heating rates.

[11]. The decrease of maximum diameter for the same alloy may be attributed to the unlike casting conditions. However, it should be noted that Ishimaru et al. [10] revealed that the as-cast $Ti_{41.5}Zr_{2.5}Hf_5Cu_{42.5}Ni_{7.5}Si_1$ alloy with a diameter of 3 mm contained nanocrystals with a size of 10 nm.

Knowledge of the crystallization behaviors is of importance in evaluating the GFA as well as thermal stability of an alloy. Crystallization process of the glassy alloys can be monitored during continuous heating with a fixed heating rate. Fig. 4 displays the DSC curves of $Ti_{41.5}Zr_{2.5}Hf_5Cu_{42.5}Ni_{7.5}Si_1$ and $Ti_{41.5}Zr_{2.5}Hf_5Cu_{37.5}Ni_{7.5}Si_1Sn_5$ alloys performed at different

heating rates of 20, 40, 60, 80, 100 K/min. Note that the first crystallization peak is sensitive to the heating rate, its area and intensity increase with increasing heating rate. Furthermore, both the glass transition temperatures and the crystallization temperatures of the alloys depend on the heating rates during continuous heating. It can be seen that the glass transition temperature, T_g, and the first peak temperature of crystallization, T_{p1}, both shift to lower temperatures with decreasing heating rates. The supercooled liquid region evaluated at low heating rate is smaller than that evaluated at high heating rate, i.e., $\Delta T_x = 71.96$ K at 100 K/min, while $\Delta T_x = 64.19$ K at 20 K/min for the alloy containing 5% Sn.

The activation energy E is one of the most important kinetic parameters for the crystallization processes of a glassy alloy. DSC curves taken at different heating rates were used to determine activation energy for crystallization by following the Kissinger analysis [16,17]. Activation energy for the process can be evaluated from the heating rate dependence of the characteristic temperature as described in Kissinger equation [16]:

$$\ln\left(\frac{B}{T^2}\right) = -\frac{E}{RT} + \text{constant} \quad (2)$$

where R is the gas constant, B the heating rate, T the specific absolute temperature and E is the activation energy for the process. By plotting $\ln(B/T^2)$ against $1/(RT)$, an approximately straight line with a slope of E_g, E_x or E_{p1} will be obtained. Three different thermodynamic temperatures, i.e., the glass transition temperature, T_g, the onset temperature of crystallization, T_x, and the first peak temperature of crystallization, T_{p1}, as the specific temperatures are used to evaluate the activation energy of amorphous Sn-free and 5% Sn alloys in the present work. The plots of $\ln(B/T^2)$ against $1/(RT)$ obtained from the above three temperatures are shown in Fig. 5. The obtained activation energies E_g, E_x, and E_{p1} for Sn-free alloy are calculated to be 399.84, 261.22, 284.06 kJ/mol, respectively, while the E_g, E_x, and E_{p1} for 5% Sn alloy are calculated to be 409.51, 296.06, 302.30 kJ/mol, respectively. From the activation energy results, a conclusion can be obtained that the activation energy derived from the Kissinger plots for glass transition E_g is higher than that for crystallization E_p and E_x calculated for the peak crystallization temperature T_p and onset temperature of crystallization T_x during the continuous heating process. At the same time, the activation energy of crystallization for Sn-free alloy is greatly smaller than the value for the alloy containing 5% Sn element, revealing that the proper substitution of Cu by Sn can enhance the thermal stability against crystallization for the Ti–Zr–Hf–Cu–Ni–Si alloy.

In the present study, the interesting result was obtained that the GFA of the Ti–Zr–Hf–Cu–Ni–Si alloy was greatly improved by 5% Sn addition. The maximum diameter of the glassy rod-like sample increases from about 2 mm for $Ti_{41.5}Zr_{2.5}Hf_5Cu_{42.5}Ni_{7.5}Si_1$ alloy to 6 mm for $Ti_{41.5}Zr_{2.5}Hf_5Cu_{37.5}Ni_{7.5}Si_1Sn_5$ alloy. The high GFA in Ti–Zr–Hf–Cu–Ni–Si–Sn alloy can be explained by the following factors. First, the increase of GFA after the partial replacement of Cu by Sn in the amorphous $Ti_{41.5}Zr_{2.5}Hf_5Cu_{42.5}Ni_{7.5}Si_1$ alloy may be due to the strong interaction between Ti and Sn. Heat of mixing for Ti–Sn pairs in liquid phase is −21 kJ/mol, which is significantly larger than −9 kJ/mol for Ti–Cu. The strong interaction between Ti and Sn can promote the formation of Ti–Sn bonds in liquid phase, which can decrease the diffusivities of constituting elements and increase the liquid viscosity [18]. Second, the enhanced GFA is related to the increased packing density due to the addition of Sn [19]. The atomic radius of Sn is 0.1580 nm, which is significantly larger than 0.1280, 0.1470, 0.1250, 0.1170 nm for Cu, Ti, Ni and Si, respectively. The large difference in atomic size between Sn and the constituting elements is effective to increase the atomic packing density. Moreover, the addition of Sn follows the "confusion rule" [20], leading to a higher order multi-component system (from six components to seven components). It is generally believed that the higher the packing density, the higher the thermal stability and the higher the resistance of the supercooled liquid against crystallization [3]. Therefore, the increasing of packing density induced by minor Sn addition results in a strikingly enhanced GFA as well as thermal stability in the $Ti_{41.5}Zr_{2.5}Hf_5Cu_{37.5}Ni_{7.5}Si_1Sn_5$ alloy.

Since Ti-based metal glasses are of scientific and commercial interest due to their high specific strength, we also examined the mechanical properties of the $Ti_{41.5}Zr_{2.5}Hf_5Cu_{37.5}Ni_{7.5}Si_1Sn_5$ glassy alloy. Uniaxial compression test was conducted on

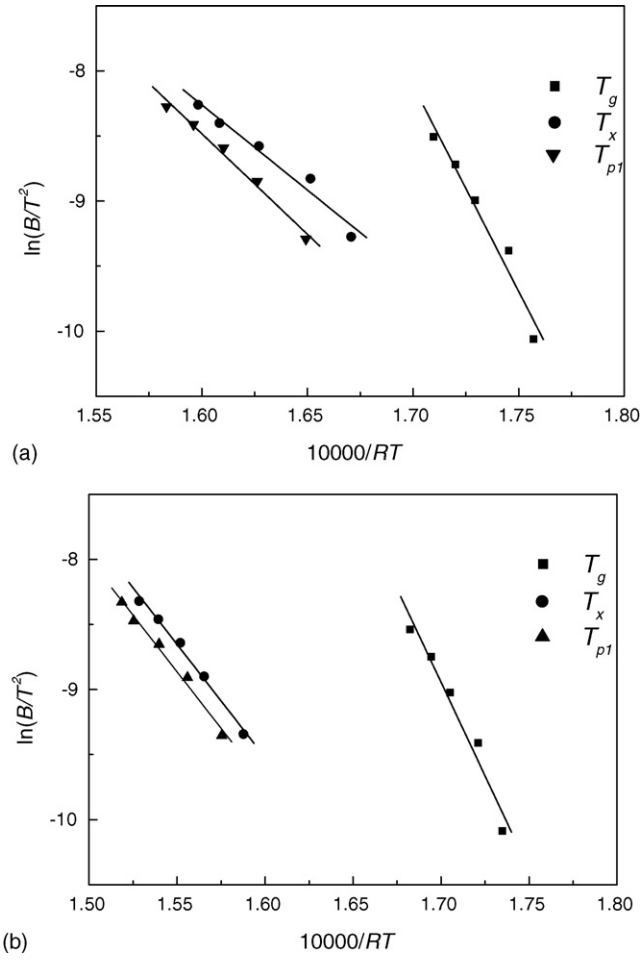

Fig. 5. Kissinger plots of DSC data for $Ti_{41.5}Zr_{2.5}Hf_5Cu_{42.5}Ni_{7.5}Si_1$ (a) and $Ti_{41.5}Zr_{2.5}Hf_5Cu_{37.5}Ni_{7.5}Si_1Sn_5$ (b) amorphous alloys.

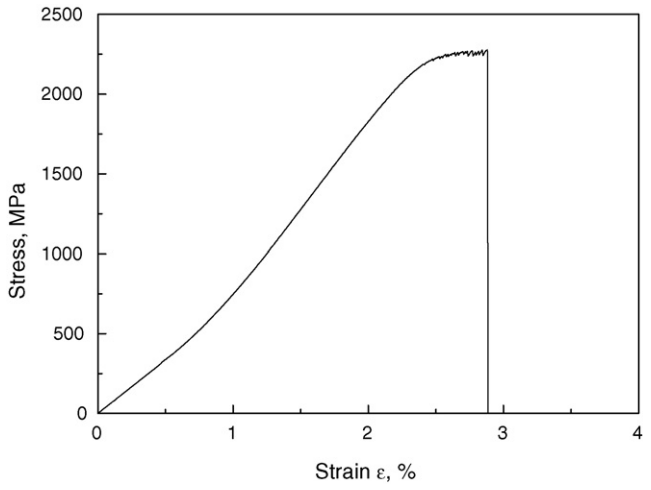

Fig. 6. Nominal compressive stress–strain curve of the $Ti_{41.5}Zr_{2.5}Hf_5Cu_{37.5}Ni_{7.5}Si_1Sn_5$ glassy alloy rod under an initial strain rate of 4×10^{-4}/s.

$Ti_{41.5}Zr_{2.5}Hf_5Cu_{37.5}Ni_{7.5}Si_1Sn_5$ glassy alloy rod with a diameter of 3 mm. Nominal compressive stress-strain curve of the $Ti_{41.5}Zr_{2.5}Hf_5Cu_{37.5}Ni_{7.5}Si_1Sn_5$ glassy alloy rod is shown in Fig. 6. It is seen that the alloy exhibits an elastic elongation of about 2.3%, followed by plastic elongation of about 0.5%, and then final fracture. The compressive fracture strength, Vickers hardness (H_v), and density are measured to be 2260 MPa, 676 kg/mm^2 and 7.0 g/cm^3, respectively. As a result, the specific strength (the ratio of strength to density) of the alloy is calculated to be 3.31×10^5 N m/kg. It is worthwhile to notice that the amorphous $Ti_{41.5}Zr_{2.5}Hf_5Cu_{37.5}Ni_{7.5}Si_1Sn_5$ alloy exhibits a higher specific strength value than Zr- [21,22], Pd- [23,24], Hf- [25], Cu- [26] and Pt- [27] based amorphous alloys. The finding of the Ti-based amorphous alloy having good mechanical properties and high thermal stability of the supercooled liquid against crystallization satisfies the requirement for the bulk amorphous alloys with high specific strength and promotes the potential for commercial applications.

4. Conclusion

We investigated the glass forming ability of the $Ti_{41.5}Zr_{2.5}Hf_5Cu_{42.5-x}Ni_{7.5}Si_1Sn_x$ alloys ($x = 0$, 1, 3, 5, 7). The amorphous $Ti_{41.5}Zr_{2.5}Hf_5Cu_{37.5}Ni_{7.5}Si_1Sn_5$ alloy exhibits a maximum diameter of 6 mm due to its high GFA. The improved GFA of amorphous $Ti_{41.5}Zr_{2.5}Hf_5Cu_{37.5}Ni_{7.5}Si_1Sn_5$ alloy is contributed to the stronger atomic bonding nature among the constituent elements and the increasing of atomic packing density. The new alloy also exhibits a high compressive fracture strength of 2260 MPa and hardness of 676 kg/mm^2 and density of 7.0 g/cm^3.

Acknowledgement

This work was supported by the Program for New Century Excellent Talents in University (China).

References

[1] T. Zhang, A. Inoue, Mater. Trans. JIM 39 (1998) 1001.
[2] T. Zhang, A. Inoue, Mater. Trans. JIM 40 (1999) 301.
[3] T. Zhang, A. Inoue, Mater. Sci. Eng. A 304–306 (2001) 771.
[4] D.V. Louzguine, A. Inoue, J. Mater. Res. 14 (1999) 4426.
[5] M.X. Xia, C.L. Ma, H.X. Zheng, J.G. Li, Mater. Sci. Eng. A 390 (2005) 372.
[6] H. Men, S. Pang, A. Inoue, T. Zhang, Mater. Trans. JIM 46 (2005) 2218.
[7] F.Q. Guo, H.J. Wang, S.J. Poon, G.J. Shiflet, Appl. Phys. Lett. 86 (2005) 091907.
[8] Y.C. Kim, J.H. Na, J.M. Park, D.H. Kim, Y.H. Lee, W.T. Kim, Appl. Phys. Lett. 86 (2003) 3093.
[9] Y.C. Kim, W.T. Kim, D.H. Kim, Mater. Sci. Eng. A 375–377 (2004) 127.
[10] M. Ishimaru, Y. Hirotsu, S. Hata, C. Ma, N. Nishiyama, K. Amiya, A. Inoue, Phil. Mag. Lett. 85 (3) (2005) 125.
[11] C.L. Ma, H. Soejima, S. Ishihara, K. Amiya, N. Nishiyama, A. Inoue, Mater. Trans. JIM 45 (2004) 3223.
[12] D. Turnbull, Contemp. Phys. 10 (1969) 473.
[13] A. Inoue, Acta Mater. 48 (1) (2000) 279.
[14] Z.P. Lu, C.T. Liu, Acta Mater. 50 (2002) 3501.
[15] Q.J. Chen, J. Shen, H.B. Fan, J.F. Sun, Y.J. Huang, D.G. Mccartney, Chin. Phys. Lett. 22 (7) (2005) 1736.
[16] H.E. Kissinger, Anal. Chem. 29 (1957) 1702.
[17] Y.L. Gao, J. Shen, J.F. Sun, G. Wang, D.W. Xing, H.Z. Xian, B.D. Zhou, Mater. Lett. 57 (2003) 1894.
[18] Y.C. Kim, S. Yi, W.T. Kim, D.H. Kim, Mater. Sci. Forum 360–362 (2001) 67.
[19] Y.C. Kim, D.H. Bae, W.T. Kim, D.H. Kim, J. Non-cryst. Solids 325 (2003) 242.
[20] A.L. Greer, Nature 366 (1993) 2003.
[21] T. Zhang, A. Inoue, Mater. Trans. JIM 39 (1998) 1230.
[22] K. Das, A. Bandyopadhyay, Y.M. Gupta, Mater. Sci. Eng. A 394 (2005) 302.
[23] C.L. Ma, A. Inoue, Mater. Trans. JIM 43 (2002) 3266.
[24] A. Inoue, Bulk Amorphous Alloys—Preparation and Fundamental Characteristics, Trans Tech Publications Ltd., Switzerland, 1998, p. 6.
[25] X. Gu, T. Jiao, L.J. Kecskes, R.H. Woodman, C. Fan, K.T. Ramesh, T.C. Hufnagel, J. Non-cryst. Solids 317 (2003) 112.
[26] D.H. Xu, B. Lohwongwatana, G. Duan, W.L. Johnson, C. Garland, Acta Mater. 52 (2004) 2621.
[27] J. Schroers, W.L. Johnson, Phys Rev. Lett. 93 (2004) 255506.